

High-pressure Syntheses and Crystal Structures of Monoclinic B-Ho₂O₃ and Orthorhombic HoGaO₃

Stefanie A. Hering^a and Hubert Huppertz^b

^a Department Chemie und Biochemie, Ludwig-Maximilians-Universität München, Butenandtstraße 5–13 (Haus D), 81377 München, Germany

^b Institut für Allgemeine, Anorganische und Theoretische Chemie, Leopold-Franzens-Universität Innsbruck, Innrain 52a, 6020 Innsbruck, Austria

Reprint requests to H. Huppertz. E-mail: Hubert.Huppertz@uibk.ac.at

Z. Naturforsch. 2009, 64b, 1032–1040; received June 26, 2009

Monoclinic holmium sesquioxide B-Ho₂O₃ and orthorhombic holmium orthogallate HoGaO₃ were synthesized in a Walker-type multianvil apparatus under high-pressure / high-temperature conditions of 11.5 GPa / 1250 °C and 7.5 GPa / 1250 °C, respectively. Both crystal structures could be determined by single-crystal X-ray diffraction data, collected at r. t. The monoclinic holmium oxide crystallizes in the space group *C2/m* (*Z* = 6) with the parameters *a* = 1394.7(3), *b* = 350.83(7), *c* = 865.6(2) pm, β = 100.23(3)°, *R*1 = 0.0517, *wR*2 = 0.1130 (all data), and the orthorhombic compound HoGaO₃ in *Pnma* (*Z* = 4) with the parameters *a* = 553.0(2), *b* = 753.6(2), *c* = 525.4(2) pm, *R*1 = 0.0222, and *wR*2 = 0.0303 (all data).

Key words: High Pressure, Multianvil, Crystal Structure, Rare-earth Oxide, Rare-earth Gallate

Introduction

During the last years, rare-earth oxoborates have been in the focus of our preparative investigations under high-pressure / high-temperature conditions. We obtained a large variety of new compositions like α -/ β -RE₂B₄O₉ (*RE* = Nd, Sm–Ho [1–3]), RE₄B₆O₁₅ (*RE* = Dy, Ho [4–6]), RE₃B₅O₁₂ (*RE* = Tm–Lu [7]), and Pr₄B₁₀O₂₁ [8], which were only attainable under high-pressure conditions. Recently, we tried to expand our research activities into the field of rare-earth gallates, using high pressure as a tool to explore new synthetic fields.

High-pressure / high-temperature investigations in the systems RE–Ga–O were started with different reactions of the rare-earth oxides RE₂O₃ (*RE* = La, Ce, Dy–Lu) with β -Ga₂O₃ in the stoichiometric ratios 1:6, 1:1, and 10:1. Using cubic Ho₂O₃ (C-Ho₂O₃) as the rare-earth oxide, we failed to observe a new compound up to now, but we obtained the high-pressure modification B-Ho₂O₃ (monoclinic) and the orthorhombic holmium orthogallate HoGaO₃. Both compounds are known from the literature. The structural characterizations of monoclinic B-Ho₂O₃, synthesized by Hoekstra [9, 10], and of HoGaO₃ (Marezio *et al.* [11, 12]), were only based on powder diffraction data. Our high-pressure / high-temperature inves-

tigations led to highly crystalline samples, which enabled us for the first time to isolate single crystals of B-Ho₂O₃ and HoGaO₃. Once again, enhancing the degree of crystallinity by high pressure during the syntheses (pressure-induced crystallization) proved to be successful, as it already was the case in the syntheses of β -SnB₄O₇ [13] and β -MB₂O₅ (*M* = Zr, Hf) [14, 15].

In this work, we report the high-pressure / high-temperature syntheses and structural data, based on single-crystal determinations, of monoclinic B-Ho₂O₃ and orthorhombic HoGaO₃. Recently, Wu *et al.* published theoretical calculations of the phase polymorphism of the rare-earth sesquioxides [16]. Their results, obtained by DFT methods, are compared with our experimental data.

Experimental Section

Syntheses

Our original intention was to synthesize rare-earth gallates with new compositions. We started with a stoichiometric ratio of C-Ho₂O₃ : β -Ga₂O₃ = 6:1. Starting materials were fine powders of cubic Ho₂O₃ (Alfa Aesar, Emmerich, Germany, 99.995 %) and β -Ga₂O₃ (Fluka, Seelze, Germany, 99.99 %), which were ground, mixed, and filled into a boron nitride crucible (Henze BNP GmbH, HeBoSint[®] S10, Kempton, Germany).

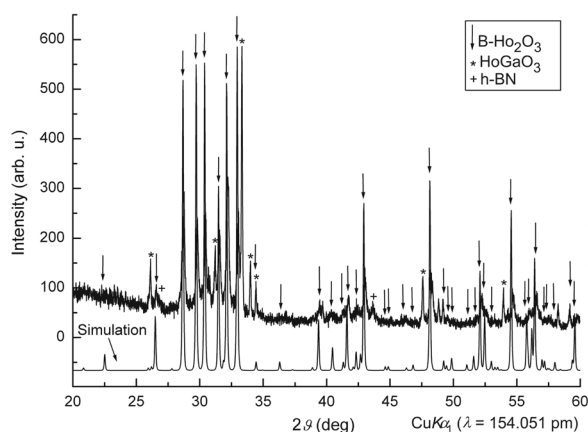


Fig. 1. Powder diffraction pattern of the reaction product from C-Ho₂O₃:β-Ga₂O₃ = 6:1 (11.5 GPa, 1250 °C). A simulation of a theoretical powder pattern of monoclinic B-Ho₂O₃, based on single-crystal data, is positioned underneath. The marked reflections refer to HoGaO₃, which occurs as a by-product. The remaining reflections correspond to residual starting material C-Ho₂O₃.

The boron nitride crucible was positioned inside the center of a 14/8-assembly, which was compressed by eight tungsten carbide cubes (TSM-10 Ceratizit, Reutte, Austria). The assembly was compressed up to 11.5 GPa in 3.5 h, using a multianvil device, based on a Walker-type module, and a 1000 t press (both devices from the company Vöggenreiter, Mainleus, Germany). A detailed description of the assembly can be found in refs. [17–19]. The sample was heated up to 1250 °C (cylindrical graphite furnace) in 15 min, kept there for 10 min, and cooled down to 650 °C in 10 min at constant pressure. Afterwards, the sample was quenched to r. t. by switching off heating, followed by a decompression period of 10.5 h. The product, a mixture of monoclinic B-Ho₂O₃ and orthorhombic HoGaO₃ as by-product, was separated from the surrounding boron nitride crucible. It appeared as a dark-grey crystalline sample, which showed the alexandrite effect [20], first discovered in 1834 by the Finnish mineralogist N. G. Nordenskjöld [21]. In daylight, the sample had a light beige/grey color; in the laboratory (neon lamps) it was brightly pink.

Fig. 1 gives a view of the powder diffraction pattern, exhibiting the lines of monoclinic B-Ho₂O₃, of HoGaO₃ as a by-product, and weak reflections of hexagonal boron nitride of the crucible, and of residual starting material C-Ho₂O₃. Some small air- and water-resistant crystals of B-Ho₂O₃ were isolated from the bulk sample for the single crystal structure determination.

Additional experiments under different high-pressure / high-temperature conditions led to the result that the pressure necessary for the formation of the high-pressure phase B-Ho₂O₃ can be reduced to a minimum of 7.5 GPa at temper-

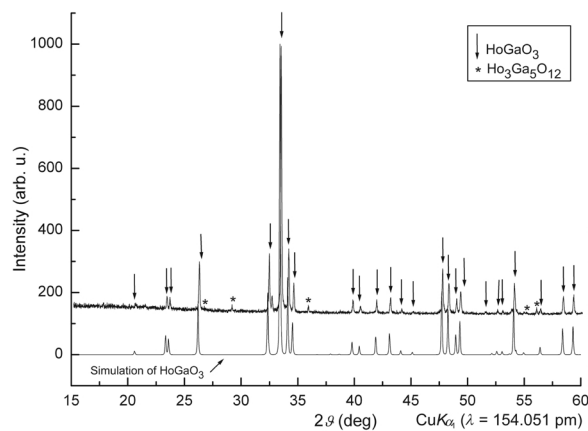


Fig. 2. Powder diffraction pattern of the reaction product HoGaO₃ synthesized from C-Ho₂O₃:β-Ga₂O₃ = 1:1 (7.5 GPa, 1250 °C). A simulation of a theoretical powder pattern of orthorhombic HoGaO₃, based on single-crystal data, is positioned underneath. The marked reflections refer to Ho₃Ga₅O₁₂ [24], which occurs as a by-product.

atures around 1250 °C. As a side effect of reduced pressure, the degree of crystallinity of the sample suffered, as often seen in the field of borates [13–15].

At this point it is important to raise the issue if pure cubic Ho₂O₃ could be transformed into the monoclinic form under these conditions. In fact, our experiments showed that it was impossible. The addition of a small amount of β-Ga₂O₃ was necessary to induce this transformation. That corresponds to the observations of Foex and Warshaw *et al.*, who added flux materials for the transformation [22, 23].

The synthesis of orthorhombic HoGaO₃ started from cubic Ho₂O₃ (Alfa Aesar, Emmerich, Germany, 99.995 %) and β-Ga₂O₃ (Fluka, Seelze, Germany, 99.99 %) in a stoichiometric ratio of C-Ho₂O₃:β-Ga₂O₃ = 1:1. Both compounds were ground up and filled into a boron nitride crucible. The experimental setup was alike the former one, except for a larger sized 18/11-assembly [17–19]. The reaction of the oxides to the rare-earth gallate HoGaO₃ occurs at a pressure of 7.5 GPa and a temperature of 1250 °C. The assembly was compressed within 3 h, followed by the heating period, in which the sample was heated up to 1250 °C within 15 min. The temperature was held for 15 min and afterwards reduced to 650 °C within 20 min. Finally, the heating was stopped in order to cool down the sample to r. t. Afterwards, the decompression to ambient pressure took 9 h. After removing the boron nitride crucible, the sample was obtained as a greyly gleaming, crystalline product, which showed also the alexandrite effect [20]. The sample was insensitive to air or moisture. Fig. 2 displays the X-ray powder diffraction pattern of the product and a simulated powder pattern of HoGaO₃, based on single-crystal data. Some weak reflections of Ho₃Ga₅O₁₂ [24] indicated the presence of this by-product.

Table 1. Crystal data and structure refinement of monoclinic B-Ho₂O₃ and orthorhombic HoGaO₃.

Empirical formula	Ho ₂ O ₃	HoGaO ₃
Molar mass, g mol ⁻¹	377.86	282.65
Crystal system	monoclinic	orthorhombic
Space group	<i>C2/m</i> (no. 12)	<i>Pnma</i> (no. 62)
Powder diffractometer	Stoe Stadi P	
Radiation	CuK _{α1} (λ = 154.051 pm)	
Powder data		
<i>a</i> , pm	1394.3(7)	554.11(4)
<i>b</i> , pm	350.0(3)	756.0(2)
<i>c</i> , pm	864.4(8)	527.75(9)
β, deg	100.18(7)	
<i>V</i> , nm ³	0.4151(4)	0.21891(8)
Single-crystal diffractometer	Enraf-Nonius	Stoe IPDS
Radiation	Kappa CCD	
	MoK _{α1} (λ = 71.073 pm)	
	(graphite monochromator)	
Single-crystal data		
<i>a</i> , pm	1394.7(3)	553.0(2)
<i>b</i> , pm	350.83(7)	753.6(2)
<i>c</i> , pm	865.6(2)	525.4(2)
β, deg	100.23(3)	
<i>V</i> , nm ³	0.4168(2)	0.21891(8)
Formula units per cell	<i>Z</i> = 6	<i>Z</i> = 4
Calculated density, g cm ⁻³	9.03	8.58
Crystal size, mm ³	0.02 × 0.02 × 0.02	0.04 × 0.02 × 0.02
Temperature, K	293(2)	293(2)
Detector distance, mm	40.0	40.0
Exposure time, min	20.0	25.0
Absorption coeff., mm ⁻¹	56.3	47.9
<i>F</i> (000), e	948	488
θ range, deg	3.5–30.0	4.7–30.0
Range in <i>hkl</i>	±19; ±4; ±12	±7; ±10; ±7
Total reflections	3514	2057
Independent reflections	689	342
<i>R</i> _{int}	0.0744	0.0697
Reflections with <i>I</i> ≥ 2σ(<i>I</i>)	576	284
<i>R</i> _σ	0.0505	0.0396
Data / ref. parameters	689 / 48	342 / 29
Absorption correction	numerical	multi-scan (HABITUS (SCALEPACK [26]) TUS [30, 31])
Final <i>R1</i> / <i>wR2</i> [<i>I</i> ≥ 2σ(<i>I</i>)]	0.0425 / 0.1087	0.0156 / 0.0296
Final <i>R1</i> / <i>wR2</i> (all data)	0.0517 / 0.1130	0.0222 / 0.0303
Goodness-of-fit on <i>F</i> ²	1.041	0.854
Largest diff. peak and hole, e Å ⁻³	4.2 –4.0	1.2 –1.6

Crystal structure analyses

To analyze the product of the reaction C-Ho₂O₃:β-Ga₂O₃ = 6:1, a Stoe Stadi P powder diffractometer with monochromatized CuK_{α1} radiation was employed. The reflections of the main phase (monoclinic B-Ho₂O₃, Fig. 1) were indexed using the program routine ITO [25]. The results led to a monoclinic cell (Table 1).

Although the crystals of the phase were very small, single crystals of monoclinic B-Ho₂O₃ could be isolated from the sample by mechanical fragmentation. To check their quality,

Table 2. Atomic coordinates and isotropic equivalent displacement parameters *U*_{eq} (Å²) of B-Ho₂O₃ (space group: *C2/m*) (standard deviations in parentheses). *U*_{eq} is defined as one third of the trace of the orthogonalized *U*_{ij} tensor. The corresponding theoretical values (Wu *et al.* [16]) are shown in brackets under the measured values.

Atom	W. position	<i>x</i>	<i>y</i>	<i>z</i>	<i>U</i> _{eq}
Ho1	4 <i>i</i>	0.63508(5)	0	0.4880(2)	0.0129(3)
		[0.6347]	[0]	[0.4879]	
Ho2	4 <i>i</i>	0.68977(5)	0	0.1369(2)	0.0130(3)
		[0.6916]	[0]	[0.1371]	
Ho3	4 <i>i</i>	0.96655(5)	0	0.1869(2)	0.0150(3)
		[0.9679]	[0]	[0.1859]	
O1	4 <i>i</i>	0.1282(8)	0	0.282(2)	0.020(3)
		[0.1278]	[0]	[0.2815]	
O2	4 <i>i</i>	0.8244(8)	0	0.030(2)	0.018(3)
		[0.8254]	[0]	[0.0302]	
O3	4 <i>i</i>	0.7938(8)	0	0.373(2)	0.019(3)
		[0.7935]	[0]	[0.3768]	
O4	4 <i>i</i>	0.4695(8)	0	0.343(2)	0.015(2)
		[0.4711]	[0]	[0.3430]	
O5	2 <i>b</i>	0	1/2	0	0.012(3)
		[0]	[1/2]	[0]	

Table 3. Anisotropic displacement parameters *U*_{ij} (Å²) of B-Ho₂O₃ (space group *C2/m*) (standard deviations in parentheses, *U*₁₂ = *U*₂₃ = 0).

Atom	<i>U</i> ₁₁	<i>U</i> ₂₂	<i>U</i> ₃₃	<i>U</i> ₁₃
Ho1	0.0079(4)	0.0157(5)	0.0152(5)	0.0023(3)
Ho2	0.0093(4)	0.0147(5)	0.0154(5)	0.0040(3)
Ho3	0.0090(4)	0.0162(5)	0.0187(5)	–0.0004(3)
O1	0.010(5)	0.026(7)	0.023(7)	0.000(5)
O2	0.013(5)	0.027(7)	0.012(6)	–0.001(4)
O3	0.021(6)	0.016(7)	0.020(7)	0.000(5)
O4	0.011(5)	0.019(6)	0.016(6)	0.006(4)
O5	0.016(8)	0.013(8)	0.006(7)	–0.001(6)

the crystals were examined by a Buerger precession camera, combined with an image plate system (Fujifilm BAS-1800), to test their suitability for the intensity data collection.

Single-crystal intensity data were collected at r. t. from a small regular crystal, applying an Enraf-Nonius Kappa-CCD single-crystal diffractometer with graded multi-layer X-ray optics and MoK_{α1} radiation (λ = 71.073 pm). The lattice parameters from the single-crystal structure determination of monoclinic Ho₂O₃ (see Table 1) agree well with those of the powder pattern (Table 1). A multi-scan absorption correction (SCALEPACK [26]) was applied to the intensity data. According to the systematic reflection conditions, the space groups *C2/m* (no. 12) and *C2* (no. 5) were derived. The structure solution and the parameter refinement with anisotropic displacement parameters for all atoms (full-matrix least-squares against *F*²) were successfully achieved in the space group *C2/m* by the SHELX-97 software suite [27, 28]. All relevant information and details concerning the single-crystal data collection are listed in Table 1. Furthermore, the positional

		Table 4. Interatomic distances (pm) of B-Ho ₂ O ₃ (space group <i>C2/m</i>) based on single-crystal data (standard deviations in parentheses).
Ho1–O4	224(2)	
Ho1–O3	225.6(8) 2×	
Ho1–O4	243(2)	
Ho1–O1	249(2) 2×	
Ho1–O3	258(2)	
Ho2–O2	224(2)	
Ho2–O2	225.7(8) 2×	
Ho2–O3	229(2)	
Ho2–O1	240.5(9) 2×	
Ho2–O1	270(2)	
Ho3–O2	219.7(2)	
Ho3–O4	220.8(7) 2×	
Ho3–O1	226.1(2)	
Ho3–O5	248.58(7) 2×	

Table 5. Atomic coordinates and isotropic equivalent displacement parameters U_{eq} (\AA^2) of HoGaO₃ (space group: *Pnma*) (standard deviations in parentheses). U_{eq} is defined as one third of the trace of the orthogonalized U_{ij} tensor.

Atom	W. position	x	y	z	U_{eq}
Ho1	4c	0.56586(5)	1/4	0.01685(5)	0.005(2)
Ga1	4a	0	1/2	0	0.0044(2)
O1	4c	0.0356(9)	3/4	0.1030(8)	0.0065(9)
O2	8d	0.1973(6)	0.5542(5)	0.6941(6)	0.0067(7)

Table 6. Anisotropic displacement parameters U_{ij} (\AA^2) of HoGaO₃ (space group *Pnma*) (standard deviations in parentheses).

Atom	U_{11}	U_{22}	U_{33}	U_{23}	U_{13}	U_{12}
Ho1	0.0036(2)	0.0061(2)	0.0058(2)	0	0.0002(2)	0
Ga1	0.0033(3)	0.0053(3)	0.0045(3)	0.0000(2)	0.0001(2)	−0.0003(2)
O1	0.002(2)	0.009(2)	0.008(2)	0	0.001(2)	0
O2	0.004(2)	0.001(2)	0.007(2)	0.000(2)	−0.001(2)	0.001(2)

Table 7. Interatomic distances (pm), calculated with the single-crystal lattice parameters of HoGaO₃ (standard deviations in parentheses).

Ho1–O1	224.6(4)		Ho1–O2	227.2(4)	2×
Ho1–O1	229.2(5)		Ho1–O2	248.9(4)	2×
Ho1–O2	264.8(4)	2×			
Ga1–O1	197.0(2)	2×	Ga1–O2	198.5(3)	2×
Ga1–O2	200.2(3)	2×			

parameters (Table 2), anisotropic displacement parameters (Table 3) and interatomic distances (Table 4) are recorded.

The product of the reaction between cubic C-Ho₂O₃ and β -Ga₂O₃ (ratio: 1 : 1), leading to orthorhombic HoGaO₃, was also examined with a Stoe Stadi P diffractometer with monochromatized $\text{CuK}\alpha_1$ radiation ($\lambda = 154.051$ pm). The indexing of the powder diffraction pattern (Fig. 2) of HoGaO₃ with the program TREOR [29] resulted in an orthorhombic unit cell (see Table 1). Single-crystals of HoGaO₃ were mechanically separated and isolated in order to examine the crystals with a Buerger precession camera and an image plate system (Fujifilm BAS-1800). The size of one single crystal was sufficient for the data collection

on a Stoe IPDS-I diffractometer ($\text{MoK}\alpha_1$ radiation: $\lambda = 71.073$ pm). The single-crystal intensity data were collected at r. t. A numerical absorption correction (HABITUS [30, 31]) was applied to the intensity data. The systematic reflection conditions led to the space groups *Pnma* (no. 62) and *Pna2₁* (no. 33). The structure solution and the parameter refinement with anisotropic displacement parameters for all atoms (full-matrix least-squares against F^2) were successfully achieved in the space group *Pnma*, using the SHELX-97 software suite [27, 28]. All relevant information and details concerning the data collection of orthorhombic HoGaO₃ are listed in Table 1. The positional parameters (Table 5), anisotropic displacement parameters (Table 6), and interatomic distances (Table 7) of HoGaO₃ are listed in the designated Tables.

Further details of the crystal structure investigations may be obtained from Fachinformationszentrum Karlsruhe, 76344 Eggenstein-Leopoldshafen, Germany (fax: +49-7247-808-666; e-mail: crysdata@fiz-karlsruhe.de, http://www.fiz-informationsdienste.de/en/DB/icsd/depot_anforderung.html) on quoting the deposition numbers CSD-420710 (B-Ho₂O₃) and CSD-420711 (HoGaO₃).

Results and Discussion

B-Ho₂O₃

Rare-earth sesquioxides are of high interest. About 80 years ago, Goldschmidt *et al.* [32] started to examine this sector. They classified these oxides in A-*RE*₂O₃, B-*RE*₂O₃, and C-*RE*₂O₃ with respect to their different crystal structures. Other groups tried to find out which factors (ionic radius of the *RE*³⁺ ion, temperature, pressure) cause the formation of the specific structure type in the row of the lanthanide ions [33–35]. In detail, type A includes the rare-earth oxides from Ce to Pm, *i. e.* the “early” elements in

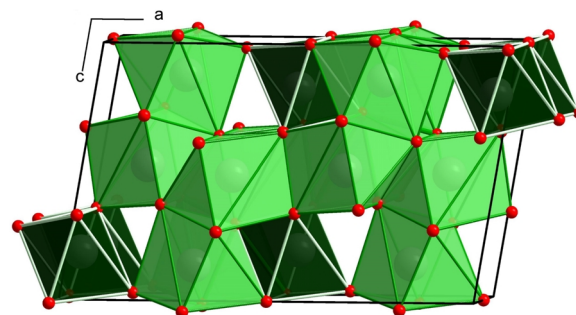


Fig. 3. (Color online). Crystal structure of monoclinic B-Ho₂O₃ viewed along $[0\bar{1}0]$. The light and dark polyhedra correspond to the capped trigonal-prismatically and octahedrally coordinated Ho³⁺ ions, respectively.

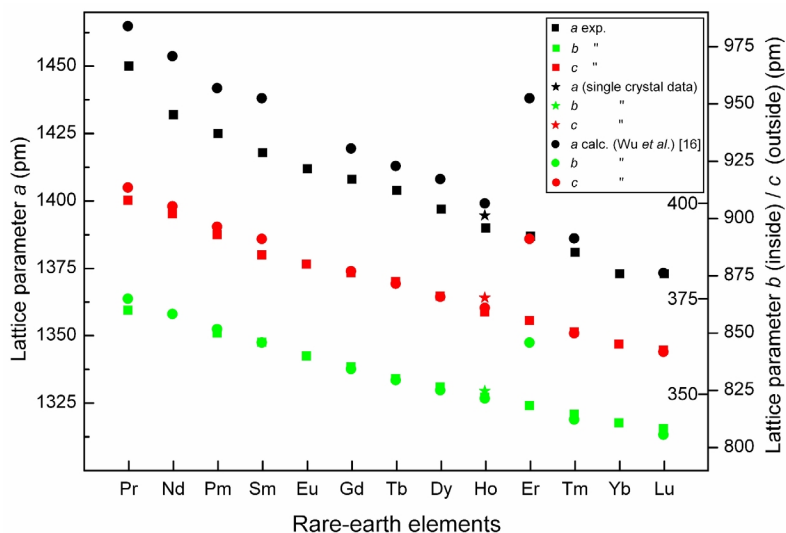


Fig. 4. (Color online). Comparison of the lattice parameters a , b , and c of the monoclinic B-type sesquioxides. The square (■) marks experimental values from the literature, the circle (●) shows data from theoretical calculations [16], and the star (*) stands for the experimental data of this work (single-crystal data).

the rare-earth series. These structures possess trigonal symmetry, crystallizing in the space group $P\bar{3}m1$ (no. 164). Often, this structure type is called the lanthanum oxide type. There are trivalent cations coordinated to seven oxygen ions. Remarkable are the different bond lengths in the coordination sphere of the rare-earth ions, which separate into four short and three long $RE-O$ distances. The monoclinic type B sesquioxides crystallize in the space group $C2/m$ (no. 12) including the sesquioxides of promethium to lutetium, where the RE^{3+} ions are surrounded by six and seven oxygen anions, forming six-vertex polyhedra (octahedra) and capped trigonal-prismatic seven-vertex polyhedra, respectively. With six- and seven-fold coordinated rare-earth cations, the structure can be described as intermediate between the cubic C-phase (only REO_6 units) and the trigonal A-phase (only REO_7 units) [36]. Fig. 3 gives a detailed view of the structure of monoclinic B-Ho₂O₃. The so-called C-type sesquioxides form cubic structures and are only found with the “late” rare-earth elements, from europium to lutetium. The structure can be described as Mn₂O₃-type (defective fluorite structure), crystallizing in the space group $Ia\bar{3}$ (no. 206).

It is noteworthy that there exist several ways of transformation between the three different rare-earth oxide phases, depending on temperature and pressure conditions [22,23]. Additional reaction components can help to transform the sesquioxides during the temperature treatment. For example, Foex *et al.* achieved a transformation from the C-type to the B-type structure

by adding some lime [33], or by offering support with oxides like CaO and SrO [37].

The high-pressure modification of holmium sesquioxide (B-Ho₂O₃) was first synthesized by Hoekstra [9,10]. He examined phase transformations in rare-earth oxides using a tetrahedral anvil high-pressure device developed by Hall [38]. It was figured out that the phase transformations of the cubic rare-earth sesquioxides into the monoclinic compounds (C-B transformation) are reversible under certain high-pressure / high-temperature conditions between 2.5 and 4 GPa at 900–1000 °C [9]. Furthermore, he was able to determine the cell parameters of the monoclinic compound B-Ho₂O₃ from powder diffraction patterns [10], leading to lattice parameters of $a = 1390(1)$, $b = 349.2(3)$, $c = 859.2(8)$ pm, and $\beta = 99.98(5)^\circ$. The indexed cell and the intensities of the reflections in the powder pattern led to the conclusion that this phase was isotypic to the structure type of monoclinic B-Sm₂O₃, published earlier by Cromer [39]. Sawyer *et al.* succeeded in transforming parts (~ 20%) of the cubic starting material C-Ho₂O₃ by high-pressure impact methods [36]. Heating of C-Ho₂O₃ at atmospheric pressure did not lead to a phase transformation [40]. Hoekstra [10] and Sawyer [36] showed that the monoclinic phase B-Ho₂O₃ disappears under temperature treatment and is transformed into the cubic phase C-Ho₂O₃, which supported the prediction of a metastable high-pressure phase [10]. Recently, Wu *et al.* [16] reported theoretical calculations on the phase transitions and lattice

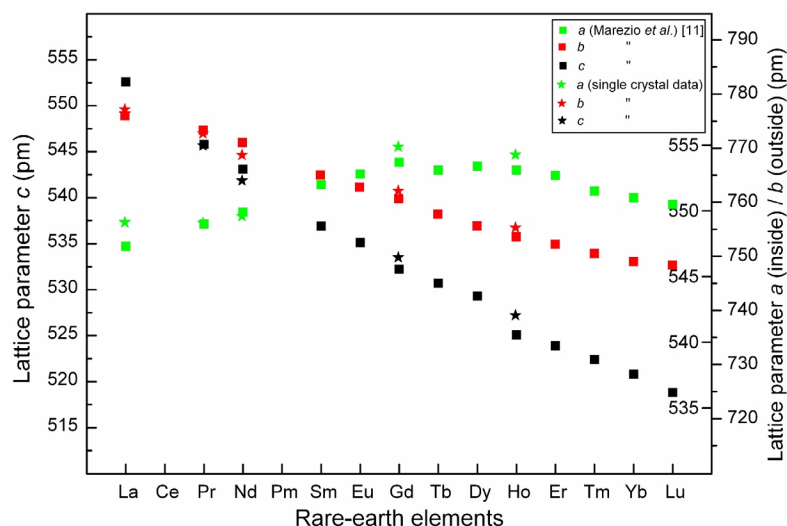


Fig. 5. (Color online). Lattice parameters a , b , and c of the different rare-earth gallates $RE\text{GaO}_3$ ($RE = \text{La, Pr, Nd, Sm-Lu}$; standard setting $Pnma$). The square stands for the literature values of Marezio *et al.* [11] and the star for the known single-crystal data.

parameters of the rare-earth sesquioxides RE_2O_3 ($RE = \text{La-Lu, Y, Sc}$) based on DFT (density functional theory) and PAW (project augmented wave) methods. A comparison of the experimental single-crystal lattice parameters ($a = 1394.7(3)$, $b = 350.83(7)$, $c = 865.6(2)$ pm, $\beta = 100.23(3)^\circ$) and atomic coordinates (Table 2) of B-Ho₂O₃ (this work) with the theoretical values obtained by Wu *et al.* [$(a_{\text{calc.}} = 1399.14$, $b_{\text{calc.}} = 348.87$, $c_{\text{calc.}} = 861.01$ pm, $\beta_{\text{calc.}} = 100.266^\circ$ [16]) and Table 2] shows good accordance. Fig. 4 presents the lattice parameters a , b , and c of the monoclinic B-type sesquioxides derived from experimental data of the literature (■), the theoretical work of Wu *et al.* (●) [16], and the experimental data of B-Ho₂O₃ from this work [single-crystal data (*)]. The lattice parameters tally well and decrease almost linearly due to the lanthanide contraction, except for the theoretical values for B-Er₂O₃ [16].

Fig. 3 shows the structure of monoclinic B-Ho₂O₃ with a view along $[0\bar{1}0]$, displaying two different types of polyhedra: distorted octahedrally coordinated Ho³⁺ ions next to sevenfold coordinated cations in the form of capped trigonal prisms. A closer look at the coordination sphere of Ho3 reveals six octahedrally arranged oxygen atoms at distances between 219.7(2) and 248.58(7) pm (av. = 230.8 pm) (Table 4), and an additional oxygen atom at a distance of 312.7 pm. MAPLE calculations (Madelung part of lattice energy) [41–43] proved a negligible coordinative contribution of $E_{\text{CoN}} = 0.003$ (effective coordination number) for this ion; so the sixfold coordinated description is

reasonable. The Ho–O distances in the capped trigonal prisms (Ho1, Ho2) are in the range between 224 and 270 pm (av. = 237.8 pm).

HoGaO₃

In the ternary system $RE\text{-Ga-O}$, four compositions are known: $RE_3\text{Ga}_5\text{O}_{12}$ ($RE = \text{Y, Sm, Gd, Dy, Ho, Yb, Lu}$; garnet structure [24, 44–48]), $RE_3\text{GaO}_6$ ($RE = \text{Nd, Sm-Er}$) [49–51], $RE_4\text{Ga}_2\text{O}_9$ ($RE = \text{La, Pr, Nd, Sm-Gd}$) [52–54], and $RE\text{GaO}_3$ ($RE = \text{La, Pr, Nd, Sm-Lu}$) [11, 12, 55–61]. The latter compounds were synthesized under atmospheric pressure or *via* decomposition of the related garnets $RE_3\text{Ga}_5\text{O}_{12}$ ($RE = \text{Sm-Lu}$) under high-pressure / high-temperature conditions in the presence of an NaOH flux [12]. In this context, HoGaO₃ was synthesized for the first time by Marezio *et al.* and characterized by the lattice parameters $a = 525.1(2)$, $b = 553.1(2)$, $c = 753.6(2)$ pm (setting: $Pbnm$) [11]. The structure was described as isostructural with the rare-earth orthoferrites, possessing an orthorhombic perovskite-like structure (GdFeO₃ type [62]). Our single-crystal data for HoGaO₃ [$a = 553.0(2)$, $b = 753.6(2)$, $c = 525.4(2)$ pm (standard setting: $Pnma$) (Table 1)] agree well with the original values of Marezio *et al.* [11]. Further single-crystal data exist only for the rare-earth orthogallates $RE\text{GaO}_3$ ($RE = \text{La, Pr, Nd, Gd}$) [58–61].

Fig. 5 shows a comparison of the different lattice parameters a , b , and c of all known rare-earth gallates in the standard setting (space group: $Pnma$) including the values of HoGaO₃. The three axes show

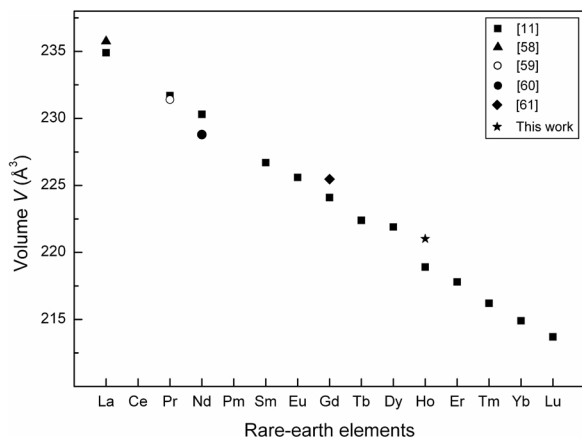


Fig. 6. Volume of the different rare-earth gallates $REGaO_3$ ($RE = La, Pr, Nd, Sm-Lu$; standard setting $Pnma$).

a different behavior: while the b and c parameters decrease smoothly on going from La to Lu, the a parameter has an unexpected behavior showing a maximum at about Gd, which was already observed by Marezio *et al.* for the rare-earth gallates [11] and by Eibschütz for the corresponding orthoferrites [63]. This effect is commonly interpreted as a consequence of the size of the rare-earth ions: as the size of RE^{3+} decreases, the average $RE^{3+}-O$ distance of the first nearest oxygen atoms decreases as well (first effect), whereas the average $RE^{3+}-O$ distance of the second nearest oxygen atoms increases (second effect). Only the a parameter is affected by this double effect, leading to an increase on going from La to Gd, because in this region the second effect is the predominant one, whereas it decreases from Gd to Lu, because here the first effect is predominant. This unsatisfactory explanation has to be checked in the future, when the missing single-crystal data in the series will become available. Similar observations were described by Berkowski *et al.*, who investigated single crystals of the solid solution $La_{1-x}Nd_xGaO_3$ [64]. It was found that the unit cell volume decreases linearly with an increasing Nd concentration according to Vegard's law. This agrees with the general behavior of all ternary rare-earth gallates, showing decreasing volumes due to the lanthanide contraction (Fig. 6). With increasing Nd concentration x in $La_{1-x}Nd_xGaO_3$, the lattice parameters a and c decrease (setting of space group $Pbnm$), whereas b increases. At $x = 0.32$, the parameters a and b become equal, and the crystal adopts a pseudo-tetragonal structure. Due to the preferred tendency for twinning, these

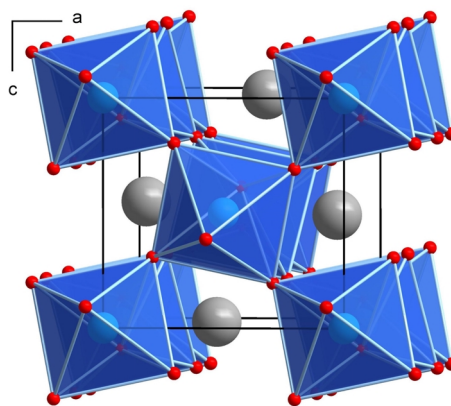


Fig. 7. (Color online). View approximately along the $[0\bar{1}0]$ axis of orthorhombic $HoGaO_3$, illustrating the GaO_6 octahedra. The Ho atoms are positioned in the resulting channels.

solid solutions were characterized by powder X-ray diffraction.

The orthogallate structure of $HoGaO_3$ crystallizes in an orthorhombically distorted perovskite-like structure ($GdFeO_3$ type), being isostructural to the rare-earth orthoferrites, investigated and described by Geller *et al.* [65, 66], Will [67], and Marezio *et al.* [68]. Fig. 7 shows the structure of the holmium orthogallate with a view along $[010]$. Like in cubic perovskite-structures, the oxygen and rare-earth ions form a face-centered cubic structure, in which the Ga^{3+} ions occupy $1/4^{th}$ of the octahedrally coordinated positions. Different from the cubic perovskite structure, the GaO_6 octahedra are distorted along the c axis and tilted against each other. The Ga–O bond lengths in $HoGaO_3$ range from 197.0(2) to 200.2(3) pm (av. = 198.6 pm) (Table 7). The distances correspond to the values found for octahedrally coordinated gallium atoms in α - Ga_2O_3 (192–208 pm [69]) and β - Ga_2O_3 (193.5(2)–207.4(1) pm [70]). The holmium cations show a 4+4 coordination, displaying Ho–O bond lengths in the ranges 224.6(4)–229.2(5) pm (the first four) and 248.9(4)–264.8(4) pm (the second four). The experimental average value of (242.0 pm) is in good accordance with the average bond length of 236 pm found in Ho_3GaO_6 [49].

Conclusions

The successful high-pressure / high-temperature synthesis and structural characterization of monoclinic holmium sesquioxide B-Ho₂O₃ and orthorhombic holmium orthogallate $HoGaO_3$ are reported in this

work. High-pressure / high-temperature conditions of 11.5 GPa / 1250 °C and 7.5 GPa / 1250 °C led to samples of B-Ho₂O₃ and HoGaO₃, respectively. Although both compounds were already known from the literature, the syntheses of samples with a high degree of crystallinity allowed structure determinations based on single-crystal data for the first time.

Acknowledgements

The authors gratefully acknowledge the continuous support of this work by Prof. Dr. W. Schnick, Department Chemie and Biochemie of the University of Munich (LMU). Special thanks go to Dr. P. Mayer and T. Miller for collecting single-crystal data. H. Huppertz is indebted to the Fonds der Chemischen Industrie for financial support.

- [1] H. Emme, H. Huppertz, *Z. Anorg. Allg. Chem.* **2002**, 628, 2165.
- [2] H. Emme, H. Huppertz, *Chem. Eur. J.* **2003**, 9, 3623.
- [3] H. Emme, H. Huppertz, *Acta Crystallogr.* **2005**, C61, i23.
- [4] H. Huppertz, B. von der Eltz, *J. Am. Chem. Soc.* **2002**, 124, 9376.
- [5] H. Huppertz, *Z. Naturforsch.* **2003**, 58b, 278.
- [6] H. Huppertz, H. Emme, *J. Phys.: Condens. Matter* **2004**, 16, 1283.
- [7] H. Emme, M. Valldor, R. Pöttgen, H. Huppertz, *Chem. Mater.* **2005**, 17, 2707.
- [8] A. Haberer, G. Heymann, H. Huppertz, *J. Solid State Chem.* **2007**, 180, 1595.
- [9] H. R. Hoekstra, *Science* **1964**, 164, 1163.
- [10] H. R. Hoekstra, *Inorg. Chem.* **1965**, 5, 754.
- [11] M. Marezio, J. P. Remeika, P. D. Dernier, *Inorg. Chem.* **1968**, 9, 1337.
- [12] M. Marezio, J. P. Remeika, P. D. Dernier, *Mater. Res. Bull.* **1966**, 1, 247.
- [13] J. S. Knyrim, F. M. Schappacher, R. Pöttgen, J. Schmedt auf der Günne, D. Johrendt, H. Huppertz, *Chem. Mater.* **2007**, 19, 254.
- [14] J. S. Knyrim, H. Huppertz, *J. Solid State Chem.* **2007**, 180, 742.
- [15] J. S. Knyrim, H. Huppertz, *Z. Naturforsch.* **2008**, 63b, 707.
- [16] B. Wu, M. Zinkevich, F. Aldinger, D. Wen, L. Chen, *J. Solid. State Chem.* **2007**, 180, 3280.
- [17] D. Walker, M. A. Carpenter, C. M. Hitch, *Am. Mineral.* **1990**, 75, 1020.
- [18] D. Walker, *Am. Mineral.* **1991**, 76, 1092.
- [19] H. Huppertz, *Z. Kristallogr.* **2004**, 219, 330.
- [20] K. Schmetzer, *Naturwissenschaften* **1978**, 65, 592.
- [21] J. Schubert, *Physikalische Effekte – Anwendungen, Beschreibungen, Tabellen*, Physik Verlag, Weinheim, **1984**.
- [22] M. Foex, *Bull. Soc. Minér. Crist.* **1965**, 88, 521.
- [23] I. Warshaw, R. Roy, *J. Phys. Chem.* **1961**, 65, 2048.
- [24] G. Patzke, R. Wartchow, M. Binnewies, *Z. Kristallogr. – NCS* **1999**, 214, 143.
- [25] J. W. Visser, *J. Appl. Crystallogr.* **1969**, 2, 89.
- [26] SCALEPACK, Z. Otwinowski, W. Minor, in *Methods in Enzymology*, Vol. 276, *Macromolecular Crystallography*, Part A (Eds.: C. W. Carter Jr., R. M. Sweet), Academic Press, New York, **1997**, pp. 307.
- [27] G. M. Sheldrick, SHELXS-97 and SHELXL-97, Program Suite for the Solution and Refinement of Crystal Structures, University of Göttingen, Göttingen (Germany) **1997**.
- [28] G. M. Sheldrick, *Acta Crystallogr.* **2008**, A64, 112.
- [29] P. E. Werner, L. Eriksson, M. Westdahl, *J. Appl. Crystallogr.* **1985**, 18, 367.
- [30] X-SHAPE (version 1.05), Stoe & Cie GmbH, Darmstadt (Germany) **1999**.
- [31] W. Herrendorf, H. Bärnighausen, HABITUS, Program for Numerical Absorption Correction, Universities of Karlsruhe and Giessen, Karlsruhe, Giessen (Germany) **1993/1997**.
- [32] V. M. Goldschmidt, F. Ulrich, T. Barth, *Math. Naturw. Kl.* **1925**, 5, 5.
- [33] M. Foex, J.-P. Traverse, *Bull. Soc. Minér. Crist.* **1966**, 89, 184.
- [34] A. Iandelli, *Gazz. Chim. Ital.* **1947**, 77, 312.
- [35] M. W. Schafer, R. Roy, *J. Amer. Ceram. Soc.* **1959**, 42, 563.
- [36] J. O. Sawyer, B. G. Hyde, L. Eyring, *Inorg. Chem.* **1965**, 4, 426.
- [37] M. Foex, *Z. Anorg. Allg. Chem.* **1965**, 337, 313.
- [38] H. T. Hall, *Rev. Sci. Instr.* **1958**, 29, 267.
- [39] D. T. Cromer, *J. Phys. Chem.* **1957**, 61, 753.
- [40] L. Eyring, B. Holmberg, *Adv. Chem. Ser.* **1963**, 39, 46.
- [41] R. Hoppe, *Angew. Chem.* **1966**, 78, 52; *Angew. Chem., Int. Ed. Engl.* **1966**, 5, 95.
- [42] R. Hoppe, *Angew. Chem.* **1970**, 82, 7; *Angew. Chem., Int. Ed. Engl.* **1970**, 9, 25.
- [43] R. Hübenthal, M. Serafin, R. Hoppe, MAPLE (version 4.0), Program for the Calculation of Distances, Angles, Effective Coordination Numbers, Coordination Spheres, and Lattice Energies, University of Giessen, Giessen (Germany) **1993**.
- [44] F. Euler, J. A. Bruce, *Acta Crystallogr.* **1965**, 19, 971.
- [45] C. D. Brandle, R. L. Brans, *J. Cryst. Growth* **1974**, 26, 169.
- [46] H. Sawada, *J. Solid State Chem.* **1997**, 132, 300.
- [47] R. C. Linares, *Solid State Commun.* **1964**, 2, 229.
- [48] J. Czocharalski, *Z. Phys. Chem.* **1917**, 92, 219.
- [49] F. S. Liu, Q. L. Liu, J. K. Lang, L. T. Lang, G. B. Song,

- J. Luo, G.H. Rao, *J. Solid State Chem.* **2004**, 177, 1796.
- [50] E. Antic-Fidancev, M. Lemaitre-Blaise, M. Lacroche, P. Porcher, J. Coutures, J. P. Coutures, *J. Alloys Compd.* **1997**, 250, 342.
- [51] J. Nicholas, J. Coutures, J. P. Coutures, B. Boudot, *J. Solid State Chem.* **1984**, 52, 101.
- [52] H. Yamane, K. Ogawam, M. Omori, T. Hirai, *J. Am. Ceram. Soc.* **1995**, 78, 2385.
- [53] T.M. Gesing, R. Uecker, J. C. Buhl, *Z. Kristallogr. – NCS* **1999**, 214, 431.
- [54] F.S. Liu, Q.L. Liu, J.K. Liang, G.B. Song, J. Luo, L.T. Yang, Y. Zhang, G.H. Rao, *J. Alloys Compd.* **2004**, 381, 26.
- [55] S. Geller, *Acta Crystallogr.* **1957**, 10, 243.
- [56] J.C. Guitel, M. Marezio, J. Mareschal, *Mater. Res. Bull.* **1976**, 11, 739.
- [57] S.J. Schneider, R. S. Roth, J. L. Waring, *J. Res. Natl. Bur. Std. A* **1961**, 65, 345.
- [58] R.J. Angel, J. Zhao, N.L. Ross, C.V. Jakeways, S. A. T. Redfern, M. Berkowski, *J. Solid State Chem.* **2007**, 180, 3408.
- [59] L. Vasylechko, Ye. Pivak, A. Senyshyn, D. Savytskii, M. Berkowski, H. Borrmann, M. Knapp, C. Paulmann, *J. Solid State Chem.* **2005**, 178, 270.
- [60] L. Vasylechko, L. Akselrud, W. Morgenroth, U. Bismayer, A. Matkovskii, D. Savytskii, *J. Alloys Compd.* **2000**, 297, 46.
- [61] J. C. Guitel, M. Marezio, J. Mareschal, *Mater. Res. Bull.* **1976**, 11, 739.
- [62] P. Coppens, M. Eibschütz, *Acta Crystallogr.* **1965**, 19, 524.
- [63] M. Eibschütz, *Acta Crystallogr.* **1965**, 19, 337.
- [64] M. Berkowski, J. Fink-Finowicki, W. Piekarczyk, L. Perchuc, P. Byszewski, L.O. Vasylechko, D.I. Savytskij, K. Mazur, J. Sass, E. Kowalska, J. Kapuśniak, *J. Cryst. Growth* **2000**, 209, 75.
- [65] S. Geller, *J. Chem. Phys.* **1956**, 24, 1236.
- [66] S. Geller, E. A. Wood, *Acta Crystallogr.* **1956**, 9, 563.
- [67] G. Will, *Naturwissenschaften* **1966**, 53, 609.
- [68] M. Marezio, J. P. Remeika, P. D. Dernier, *Acta Crystallogr.* **1970**, B26, 2008.
- [69] M. Marezio, J. P. Remeika, P. D. Dernier, *J. Chem. Phys.* **1967**, 46, 1862.
- [70] J. Åhman, G. Svensson, J. Albertsson, *Acta Crystallogr.* **1996**, C52, 1336.